

## *L* Fluorescent X-Ray Relative-Intensity Measurements\*

J. H. McCrary, L. V. Singman, L. H. Ziegler,  
L. D. Looney, C. M. Edmonds, and Carolyn E. Harris  
*EG & G, Incorporated, Las Vegas, Nevada 89109*  
(Received 15 November 1971)

Measured values of the relative intensities of several *L* fluorescent x rays are reported for 13 elements ranging from cerium through plutonium. A solid-state Si(Li) spectrometer and a Bragg-diffraction spectrometer were used to analyze the x-ray excited fluorescence from thin samples. Corrections were made to the measured relative intensities for sample absorption, air absorption, and spectrometer efficiency. The accuracy of the measurements varies from  $\pm 5$  to  $\pm 15\%$ . The results are compared with those from the Scofield calculations.

### INTRODUCTION

Although several measurements<sup>1-7</sup> of *L* x-ray relative intensities were made early in the century, few recent results<sup>8,9</sup> have been reported. The purpose of the present work is to provide experimental measurements of the intensities of as many of the *L* emission lines as possible relative to that of the most intense line from the same subshell for approximately every third element from  $Z = 58$  through  $Z = 94$ .

The techniques employed in this work have been described in detail elsewhere.<sup>10</sup> Thin samples were used as fluorescers in order to minimize corrections for x-ray absorption. Two spectrometers were used in these measurements. A Bragg-diffraction spectrometer with high-resolution Soller slits was used to measure  $L\alpha_2$ -to- $L\alpha_1$  ratios, to resolve as many of the  $L\beta$  peaks as possible, and to measure their intensity relative to other prominent lines from the same or from another subshell. A Si(Li) spectrometer was used to measure the relative intensities of the  $L\gamma$  line, the  $L\alpha$  doublet, the  $L\eta$  line, the  $L\beta$  complex, and the  $L\gamma$  lines.

The x-ray spectra used to excite sample fluorescence in the two spectrometers were essentially the same for a given element. They were heavily filtered and were much higher in energy than the *L* edges. The relative intensities of fluorescent *L* x rays from different subshells were found to be insensitive to slight differences in the output spectra of the two x-ray machines. Peak areas, rather than peak heights, were used in analyzing the data. Corrections for sample absorption, air absorption, and spectrometer efficiency were applied to the measured relative intensities.

### APPARATUS

The high-resolution Bragg spectrometer, the Si(Li) spectrometer, and the experimental geometries used in the present work are identical with those described in Ref. 10.

### SAMPLES

Table I is a list of the sample elements, their chemical form, and their thickness. Most of the samples were deposited on 0.0005-in. Be foils, the effect of which was negligible on the results of these experiments. The Pu sample was mounted between two layers of 0.0004-in. Ni foil for health protection. The criterion for determining the sample thickness was that it should transmit  $\sim 90\%$  of its  $L\alpha$  radiation. In most cases the actual thickness was close to this nominal value. Sample thicknesses were determined by measuring the weight and areas of the sample material deposited on the Be foil. Uniformity in thickness was assumed but was not critical. All samples were made from materials whose purity was 99% or higher.

### EXPERIMENTAL PROCEDURE

Data were taken with both spectrometers in the same manner as that described in the "Experimental Procedure" section of Ref. 10. The intensities of x-ray emission lines which lay closest together in energy were measured using the Bragg

TABLE I. Samples.

Element	Material	Material thickness (mg/cm <sup>2</sup> )
Ce	CeO <sub>2</sub>	0.5
Sm	Sm	0.5
Gd	Gd	0.89
Ho	Ho	0.53
Yb	Yb	0.48
Ta	Ta	0.52
Ir	Ir	0.67
Au	Au	0.8
Pb	Pb	0.9
Bi	Bi	1.0
Th	Th	0.99
U	U	1.05
Pu	PuO <sub>2</sub>	1.5

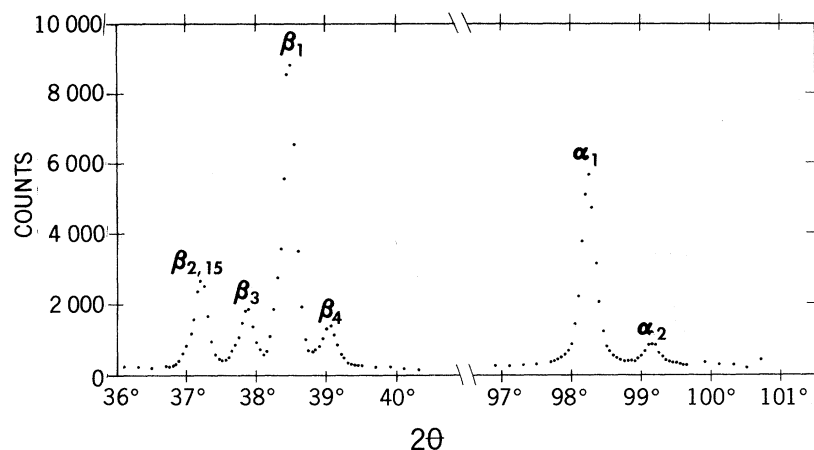


FIG. 1. Tantalum  $L$  x-ray spectrum from Bragg spectrometer (first-order diffraction from LiF for  $L\beta$  region; second-order for  $L\alpha$  region).

spectrometer. The  $L\alpha_1$  and  $L\alpha_2$  intensities were measured with this system as were the intensities of the several  $L\beta$  lines. Data were taken for each sample on both spectrometers. X-ray tube operating parameters and direct beam filtration were the same on both machines for a given sample. Negligible error was introduced into the data analysis by relating the intensities of x rays from different subshells in the two sets of data.

#### DATA ANALYSIS

All data were analyzed by adding the counts taken at equal intervals in a given peak, i. e., by using the peak area rather than the peak height. Figure 1 is a plot of the tantalum  $L$  fluorescent spectrum from the Bragg spectrometer. Some of the weaker peaks contain non-negligible contributions from neighboring peaks. Background was assumed to be a linear interpolation of the count rates well away from the peaks. After subtracting the background from all counts, the contribution from neighboring lines to the sum of the counts in a peak was estimated by assuming that each peak had the same shape and the same width.

The area of each peak was determined by adding

the counts over equal angular intervals between points where the count rate was a predetermined fraction of the peak count rate. The ratios obtained with the diffraction spectrometer were corrected for the Lorentz polarization factor and for the transmissivity of the NaI(Tl) detector window. The scintillator was opaque to the x rays for which it was used. The diffraction efficiency for a perfectly mosaic crystal is proportional to the cube of the wavelength of the radiation.<sup>11</sup> However, for the geometry used here, it is also inversely proportional to the absorption coefficient of the crystal which is very nearly proportional to the cube of the wavelength.<sup>12</sup> Hence, for the cases under consideration, the dependence of the diffraction efficiency on the wavelength very nearly vanishes and was neglected for the small wavelength separations encountered in these measurements. The Lorentz polarization correction was less than 5% for most of the  $L$  x-ray intensity ratios measured with the Bragg spectrometer. Corrections were applied for absorption of the x rays by the sample and by air, using published attenuation coefficients.<sup>13,14</sup>

Figure 2 is a plot of the  $L$  x-ray spectrum of tantalum as measured with the Si(Li) spectrometer.

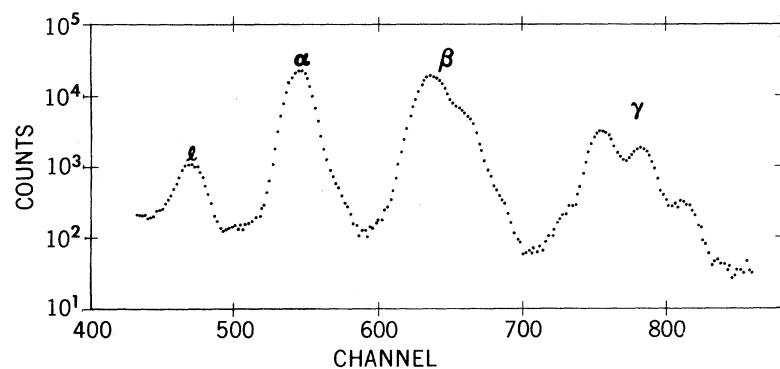


FIG. 2. Tantalum  $L$  x-ray spectrum from Si(Li) spectrometer.

TABLE II. Measured  $L_{III}$  subshell x-ray relative intensities.

Element	$\alpha_1$	$\alpha_2$	$l$	$\beta_6$	$\beta_{2,15}$	$\beta_5$
$^{58}\text{Ce}$	100	$9.8 \pm 1.5$	$4.7 \pm 0.2$		$22.4 \pm 1.5$	
$^{62}\text{Sm}$	100	$8.5 \pm 2.5$	$4.8 \pm 0.2$		$21.7 \pm 1.5$	
$^{64}\text{Gd}$	100	$12.5 \pm 1.2$	$5.2 \pm 0.2$		$19.8 \pm 1.5$	
$^{67}\text{Ho}$	100		$5.5 \pm 0.2^a$		$17.7 \pm 1.5$	
$^{70}\text{Yb}$	100	$11.9 \pm 1.2$			$22.0 \pm 1.5$	
$^{73}\text{Ta}$	100	$11.9 \pm 1.2$	$5.7 \pm 0.2$		$22.0 \pm 1.5$	
$^{77}\text{Ir}$	100	$12.6 \pm 1.2$	$6.0 \pm 0.2$			
$^{79}\text{Au}$	100	$12.3 \pm 1.2$	$6.0 \pm 0.2$	$1.3 \pm 0.2$		
$^{82}\text{Pb}$	100	$11.2 \pm 1.0$	$6.1 \pm 0.2$			
$^{83}\text{Bi}$	100	$12.5 \pm 1.0$	$6.3 \pm 0.2$			
$^{90}\text{Th}$	100	$12.4 \pm 1.0$	$7.2 \pm 0.2$	$2.1 \pm 0.2$		
$^{92}\text{U}$	100	$11.2 \pm 1.0$	$7.4 \pm 0.2$	$2.1 \pm 0.2$	$23.3 \pm 1.5$	
$^{94}\text{Pu}$	100	$10.2 \pm 1.0$		$1.7 \pm 0.3$	$24.9 \pm 1.5$	$5.1 \pm 0.5$

<sup>a</sup>Used Scofield value of  $\alpha_2/\alpha_1$ .

The resolution of this instrument was not sufficient to separate the  $L\alpha_1$  and the  $L\alpha_2$  lines nor to resolve the  $L\beta$  lines of this element. The relative intensities of the peaks in the Si(Li) spectra were determined by subtracting the background and adding the counts in all the channels in each peak. For peaks which were not completely resolved, the contribution of one peak to another was removed in the same manner as that described above for the Bragg spectrometer. The intensities of the peaks in the Si(Li) spectra were corrected for spectrometer efficiency,<sup>10</sup> sample absorption, and air absorption.

From the ratios of the individual  $L\beta$  line intensities to the total  $L\beta$  intensity as measured with the Bragg spectrometer, and from the ratios of the total  $L\beta$  intensity to the intensities of other lines as measured with the Si(Li) spectrometer, the intensity of each  $L\beta$  line relative to the strongest line from its subshell was calculated. This technique of analyzing the data is justified by the fact that the incident-beam spectra in both spec-

trometers were the same.

### RESULTS

The results of the present measurements are listed in Tables II–IV. Figure 3 is a plot of the measured  $L\alpha_2/L\alpha_1$  intensity ratios as a function of atomic number and of the theoretical ratios of Scofield.<sup>15</sup> The samarium experimental point ( $Z=62$ ) contains a large error due to the relatively poor spectrometer resolution associated with the highest diffraction order available for that measurement. Figure 4 is a plot of the  $Ll/L\alpha_1$  intensity ratios as a function of atomic number. The measured ratios average about 9% higher than the corresponding theoretical values.

The present results are in good agreement with the work of Salem *et al.*<sup>8</sup> and with the Pu measurements of Salgueiro *et al.*<sup>9</sup> There are, however, consistent differences between the present results and the Scofield calculations for the  $Ll/L\alpha_1$  and the  $L\beta_{2,15}/L\alpha_1$  ratios. The vacancies in the tables are necessitated by insufficient resolution or by in-

TABLE III. Measured  $L_{II}$  subshell x-ray relative intensities.

Element	$\beta_1$	$\eta$	$\gamma_1$	$\gamma_5$
$^{58}\text{Ce}$	100		$16.9 \pm 1.3$	
$^{62}\text{Sm}$	100		$15.1 \pm 1.3$	
$^{64}\text{Gd}$	100		$16.4 \pm 1.3$	
$^{67}\text{Ho}$	100		$17.4 \pm 1.3$	
$^{70}\text{Yb}$	100		$18.0 \pm 1.3$	
$^{73}\text{Ta}$	100		$16.8 \pm 1.3$	$0.86 \pm 0.10$
$^{77}\text{Ir}$	100	$3.4 \pm 0.4$	$20.0 \pm 1.4$	$0.75 \pm 0.09$
$^{79}\text{Au}$	100	$2.9 \pm 0.2$	$19.1 \pm 1.3$	$1.04 \pm 0.15$
$^{82}\text{Pb}$		100	$680 \pm 70$	$36 \pm 5$
$^{83}\text{Bi}$		100	$670 \pm 70$	$39 \pm 6$
$^{90}\text{Th}$	100	$3.0 \pm 0.2$	$21.0 \pm 1.4$	$1.07 \pm 0.15$
$^{92}\text{U}$	100	$2.9 \pm 0.2$	$20.9 \pm 1.5$	$1.22 \pm 0.15$
$^{94}\text{Pu}$	100	$2.8 \pm 0.4$	$21.6 \pm 1.5$	$1.32 \pm 0.15$

TABLE IV. Measured  $L_I$  subshell x-ray relative intensities.

Element	$\beta_3$	$\beta_4$	$\gamma_{2,3}$	$\gamma_{4/1,4/2}$
$^{58}\text{Ce}$				
$^{62}\text{Sm}$				
$^{64}\text{Gd}$				
$^{67}\text{Ho}$	100	$66 \pm 7$	$44 \pm 6$	$7.1 \pm 0.8$
$^{70}\text{Yb}$	100	$74 \pm 6$	$52 \pm 7$	$6.1 \pm 0.7$
$^{73}\text{Ta}$	100	$82 \pm 6$	$60 \pm 6$	$8.6 \pm 0.8$
$^{77}\text{Ir}$		100	$61 \pm 7$	$11 \pm 1$
$^{79}\text{Au}$		100		$11 \pm 1$
$^{82}\text{Pb}$	100	$97 \pm 7$		$11 \pm 1$
$^{83}\text{Bi}$	100	$88 \pm 7$		$11.6 \pm 1.5$
$^{90}\text{Th}$	100			$17 \pm 3$
$^{92}\text{U}$	100	$133 \pm 13$		$13.3 \pm 1.5$
$^{94}\text{Pu}$	100	$123 \pm 9$		$21 \pm 3$

interference between incident x-ray beam spectral impurities and sample fluorescence.

### ERRORS

Possible sources of error in these measurements include: (i) analysis of unresolved peaks, (ii) background determinations, (iii) spectrometer efficiency, (iv) sample and air absorption, (v) counting statistics, and (vi) different population of subshells in different spectrometers. Of these, the first two are the most important. These errors and estimates of their magnitude will be discussed below.

(i) *Analysis of unresolved peaks.* The same technique was used in analyzing unresolved peaks in the results from both spectrometers. The criterion was to construct two peaks with the same shape whose sum was the unresolved profile shown in the spectrum. All counts contained within each peak were added to give the relative intensity of that peak.

(ii) *Background determinations.* In analyzing the data from both spectrometers, the background count rate under the peaks was interpolated from the count rates measured away from the peaks. In most of the measurements the background count rate was less than 10% of the peak count rate. The combined error introduced into the measured relative intensities due to background determination and the analysis of unresolved peaks is estimated to be  $\pm 10\%$  for the  $L_{\alpha_2}/L_{\alpha_1}$  ratios and  $\pm 3$  to  $\pm 15\%$  for the other ratios.

(iii) *Spectrometer efficiency.* Since the correc-

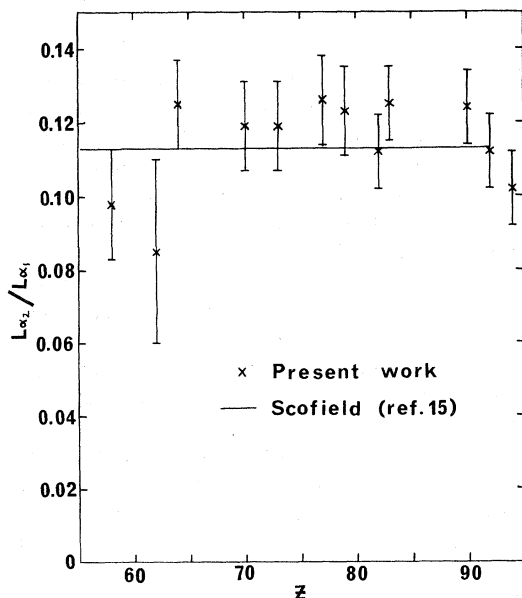


FIG. 3. Measured and theoretical values of  $L_{\alpha_2}/L_{\alpha_1}$  vs atomic number  $Z$ .

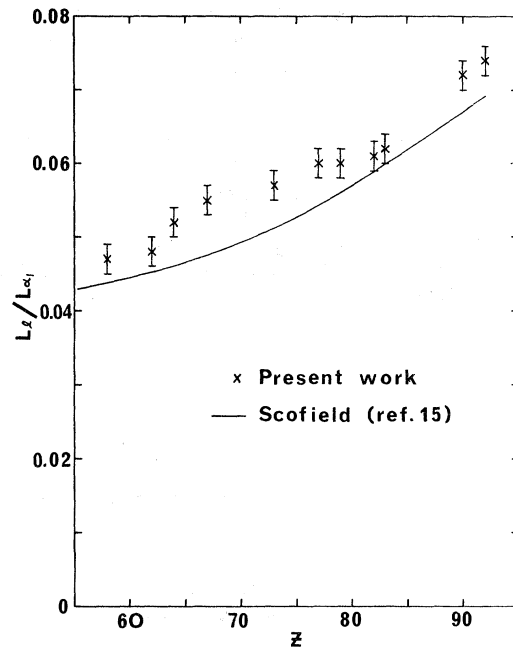


FIG. 4. Measured and theoretical values of  $L_{\beta}/L_{\alpha_1}$  vs atomic number  $Z$ .

tions for spectrometer efficiency were small (1–5%) for the Bragg spectrometer, the error in the measured ratios due to the application of this correction is negligible ( $< 1\%$ ). The ratios obtained in the higher-energy (low-efficiency) region of the solid-state spectrometer could contain errors of as much as  $\pm 2\%$ .

(iv) *Sample and air absorption.* Corrections to the measured ratios for absorption of x rays by the sample and by air were in nearly all cases less than 10%. Errors due to these corrections are believed to be less than  $\pm 1\%$  for all reported ratios.

(v) *Counting statistics.* Counting statistics introduced negligible error into most of the measurements.

(vi) *Subshell population.* Since the incident x-ray spectra were the same in both spectrometers, and since intensity ratios of x rays from different subshells are not strongly dependent upon the incident spectrum, the error introduced into the measured ratios by differences in subshell populations is believed to be negligible.

The total combined error was estimated for each measured ratio and is listed with that ratio in Table II.

### ACKNOWLEDGMENTS

The authors wish to express their appreciation to D. W. Lier and J. G. Povelites of the Los Alamos Scientific Laboratory for making possible the use of the plutonium sample.

- \*Work performed under the auspices of the U. S. AEC.  
<sup>1</sup>W. Duane and R. A. Patterson, Proc. Natl. Acad. Sci. U. S. **6**, 518 (1920); **8**, 85 (1922).  
<sup>2</sup>S. K. Allison and A. H. Armstrong, Phys. Rev. **26**, 714 (1925).  
<sup>3</sup>S. K. Allison, Phys. Rev. **30**, 245 (1927); **32**, 1 (1928).  
<sup>4</sup>A. Jönsson, Z. Physik **36**, 426 (1926).  
<sup>5</sup>V. Hicks, Phys. Rev. **36**, 1273 (1930).  
<sup>6</sup>V. J. Andrew, Phys. Rev. **42**, 591 (1932).  
<sup>7</sup>M. Botzkes, Z. Physik **89**, 667 (1934).  
<sup>8</sup>S. I. Salem, R. T. Tsutsui, and B. A. Rabbani, Phys. Rev. A **4**, 1728 (1971).  
<sup>9</sup>L. Salgueiro, J. G. Ferreira, J. J. H. Park, and M. A. S. Ross, Proc. Phys. Soc. (London) **77**, 657 (1960).  
<sup>10</sup>J. H. McCrary, L. V. Singman, L. H. Ziegler, L. D. Looney, C. M. Edmonds, and C. E. Harris, Phys. Rev. A **4**, 1745 (1971).  
<sup>11</sup>R. W. James, *The Optical Principles of the Diffraction of X Rays* (Cornell U. P., Ithaca, N. Y., 1965).  
<sup>12</sup>*International Tables for X-Ray Crystallography*, (Kynock, Birmingham, England, 1968), Vol. III.  
<sup>13</sup>J. H. McCrary, L. D. Looney, C. P. Constanten, and H. F. Atwater, Phys. Rev. A **2**, 2489 (1970).  
<sup>14</sup>E. Storm and H. I. Israel, Nucl. Data Tables, A **7**, 565 (1970).  
<sup>15</sup>J. H. Scofield, Phys. Rev. **179**, 9 (1969).

PHYSICAL REVIEW A

VOLUME 5, NUMBER 4

APRIL 1972

## Production (in Mg Vapor) and Loss (in H<sub>2</sub> Gas) of 1- to 42-keV/Nucleon X<sup>1</sup>Σ<sub>g</sub><sup>+</sup> and c<sup>3</sup>Π<sub>u</sub> Hydrogen Molecules\*

Thomas J. Morgan,<sup>†</sup> Klaus H. Berkner, and Robert V. Pyle

Lawrence Berkeley Laboratory, University of California, Berkeley, California 94720

(Received 18 November 1971)

We have investigated collisions which result in the formation and destruction of the (1sσ<sup>2</sup>)X<sup>1</sup>Σ<sub>g</sub><sup>+</sup> ground state and the (1sσ2pπ)c<sup>3</sup>Π<sub>u</sub> long-lived electronically excited state of molecular hydrogen. The molecules were formed by electron capture by 1- to 42-keV/nucleon H<sub>2</sub><sup>+</sup> or D<sub>2</sub><sup>+</sup> ions in Mg vapor. The resulting yields of H<sub>2</sub>(<sup>1</sup>Σ<sub>g</sub><sup>+</sup>), H<sub>2</sub>(<sup>3</sup>Π<sub>u</sub>), H, and H<sup>+</sup> are reported as a function of Mg-target thickness. Also reported are cross sections for total loss and ionization of the <sup>1</sup>Σ<sub>g</sub><sup>+</sup> and <sup>3</sup>Π<sub>u</sub> states of H<sub>2</sub> in collisions with H<sub>2</sub> gas.

### I. INTRODUCTION

In recent years a large amount of experimental work has been devoted to measuring excited-state populations of energetic atomic-hydrogen and helium beams, and their destruction and formation cross sections. Much less is known about energetic excited-molecular hydrogen beams. The present work extends the field of measurement of keV-energy heavy-particle collisions involving excited states to the  $n = 2$  united-atom equivalent state of molecular hydrogen. In this work we quantitatively analyze by beam-attenuation techniques the collisional formation and loss of the (1sσ<sup>2</sup>)X<sup>1</sup>Σ<sub>g</sub><sup>+</sup> ground state and the (1sσ2pπ)c<sup>3</sup>Π<sub>u</sub> long-lived electronically excited state of energetic molecular hydrogen. The energy range of the present work is from 1- to 42-keV/nucleon. The H<sub>2</sub> molecules were produced from energetic H<sub>2</sub><sup>+</sup> ions by electron capture from H<sub>2</sub> or N<sub>2</sub> gas or from Mg vapor. According to the Massey hypothesis<sup>1</sup> the maximum cross section for charge exchange is large when the energy defect is small. (The energy defect is the difference between the internal energy of the initial and final states of the collision particles.) In the case of the charge-exchange process of interest in the present experiment, i. e., H<sub>2</sub><sup>+</sup> + X → H<sub>2</sub> + . . . , the energy defect for electron capture into  $n = 2$  bound states of H<sub>2</sub> is about

4 eV for a Mg-vapor target and about 12 eV for a H<sub>2</sub> or N<sub>2</sub> gas target. Therefore, at low energies where the Massey criterion is valid, we expect Mg vapor to be a more effective charge-exchange medium for capture into excited states than H<sub>2</sub> or N<sub>2</sub> gas.

The desirability of metal vapors as charge-exchange media for the formation of excited hydrogen atoms has been experimentally verified by many groups (see, for example, Refs. 2-6). A theoretical survey of electron capture into excited states of atomic hydrogen by ground-state elements has been performed by Hiskes.<sup>7</sup> From these results Hiskes has estimated up to 50% electron capture into the <sup>3</sup>Π<sub>u</sub> state of H<sub>2</sub> by passage of H<sub>2</sub><sup>+</sup> through Mg vapor.<sup>8</sup> Based on the above considerations, Mg vapor was used to attempt to enhance the <sup>3</sup>Π<sub>u</sub> excited-state population of H<sub>2</sub> beams. In order to compare the metal-vapor results with common gases we also used H<sub>2</sub> and N<sub>2</sub> targets.

The experimental technique used for the analysis of the hydrogen molecules is the beam-attenuation technique introduced by Gilbody *et al.*<sup>9</sup> for metastable He atoms. Accurate absolute measurements can be obtained by this method only if a beam of fast projectiles contains sufficient excited particles, with long enough lifetimes and large enough cross sections to ensure observable changes in the colli-